

Development of a Clinical Type 1 Diabetes Metabolic System Model and *in Silico* Simulation Tool

Xing-Wei Wong, B.Eng,¹ J. Geoffrey Chase, Ph.D.,¹ Christopher E. Hann, Ph.D.,¹ Thomas F. Lotz, Dipl.Ing, Ph.D.,¹ Jessica Lin, B.Eng, Ph.D.,¹ Aaron J. Le Compte, B.Eng,¹ and Geoffrey M. Shaw, MbChb, FJFICM²

Abstract

Objectives:

The goal of this study was to develop a system model of type 1 diabetes for the purpose of *in silico* simulation for the prediction of long-term glycemic control outcomes.

Methods:

The system model was created and identified on a physiological cohort of virtual type 1 diabetes patients ($n = 40$). Integral-based identification was used to develop ($n = 40$) insulin sensitivity profiles.

Results:

The $n = 40$ insulin sensitivity profiles provide a driving input for virtual patient trials using the models developed. The identified models have a median (90% range) absolute percentage error of 1.33% (0.08–7.20%). The median (90% range) absolute error was 0.12 mmol/liter (0.01–0.56 mmol/liter). The model and integral-based identification of S_I captured all patient dynamics with low error, which would lead to more physiological behavior simulation.

Conclusions:

A simulation tool incorporating $n = 40$ virtual patient data sets to predict long-term glycemic control outcomes from clinical interventions was developed based on a physiological type 1 diabetes metabolic system model. The overall goal is to utilize this model and insulin sensitivity profiles to develop and optimize self-monitoring blood glucose and multiple daily injection therapy.

J Diabetes Sci Technol 2008;2(3):424-435

Author Affiliations: ¹Department of Mechanical Engineering, University of Canterbury, Christchurch, New Zealand, and ²Department of Intensive Care, Christchurch Hospital, Christchurch School of Medicine and Health Science, University of Otago, Dunedin, New Zealand

Abbreviations: (CGM) continuous glucose measurement, (CSII) continuous subcutaneous insulin infusion, (HGP) hepatic glucose production, (IDDM) insulin-dependent diabetes mellitus, (MDI) multiple daily injection, (SMBG) self-monitoring blood glucose, (TBGU) total body glucose uptake

Keywords: blood glucose, compartmental models, decision support, diabetes, hyperglycemia, insulin, simulation, subcutaneous injection

Corresponding Author: Jason Wong, Department of Mechanical Engineering, University of Canterbury, Private Bag 4800, Christchurch, New Zealand; email address xvw10@student.canterbury.ac.nz

Introduction

The control of type 1 diabetes is a widely studied and experimented research field. Previously published control methods are diverse, using different routes of insulin administration and glucose measurement. Since the 1970s, the closed-loop artificial endocrine pancreas has been heralded as the solution (as reviewed in Bequette¹). While no commercial product currently exists, the systems in current clinical use that are likely to constitute the components of an extracorporeal artificial pancreas are the continuous subcutaneous insulin infusion (CSII) pump and a continuous glucose measurement (CGM) device. Advanced control algorithms and methods to “close the loop” have also been widely studied (as reviewed elsewhere^{2–4}), despite early and ongoing limitations in sensors and pumps. Currently, the use of open-loop CGM and/or CSII has resulted in, at best, a modest *clinical* advantage over conventional methods of insulin administration or multiple daily injection (MDI) (as reviewed elsewhere^{5,6}). Additionally, these systems are only used by a small population of type 1 diabetic patients because of high upfront costs, costs of consumables, complexity, and the extensive health care infrastructure and support required. The prevalence of CSII use is as low as 2% of the type 1 diabetes population in the United Kingdom and up to 15–20% elsewhere and in the United States.⁷

Hence, there is a more practical and urgent need to address the large majority of the type 1 diabetes population using conventional glucose measurement, i.e., self-monitoring blood glucose (SMBG), and insulin administration, i.e., MDI methods, and for whom current conventional or intensive therapies are failing to deliver recommended levels of glycemic control.⁸ In the United States, over 50% of diagnosed diabetics aged 20–64 are deemed “out of control.”⁹ The higher accuracy of bedside capillary blood glucose meters^{10,11} and the latest insulin analogues for MDI therapy,¹² coupled with better control methods, have the potential to provide better care to the majority of outpatient or ambulatory type 1 diabetics than currently observed. Such techniques must necessarily be simple to implement to ensure broad clinical uptake by the diabetes population.

This study reports the development of a system model of the type 1 insulin–glucose regulatory system and its identification on a virtual patient cohort. The models utilized have several novel and unique features. In

particular, the insulin model used is unique and captures the insulin kinetics of multiple insulin types in a single pharmacokinetic model for all shared physiological spaces. The pharmacodynamic model used has not been reported previously but bears components of a similar nature to other such models used in this field due to the need to capture similar physiology. This study is the basis for a novel model-based application to develop a simple and practical adaptive method for clinical glycemic control of type 1 diabetes using multiple daily injection and self-monitoring blood glucose measurements. In addition, the modeling of long-term clinical outcomes of glycemic control and their corroboration against clinical expectations and studies are explored further in a subsequent *in silico* simulation on a virtual patient cohort, which is also reported in this issue. Later, the complex interaction of all quantifiable errors in protocol application is investigated in a Monte Carlo study to test the robustness of the developed protocol in effectiveness and safety.¹³

Model Development

The system model shown in **Equation (1)** is an evolution of the model of Chase *et al.*¹⁴ and Wong *et al.*¹⁵

$$\dot{G}(t) = EGP_{0-G} - p_G G(t) - S_I G(t) Q(t) - RGC(t) - CNS + P(t) \quad (1)$$

where $G(t)$ is plasma glucose concentration (mmol/liter), CNS is central nervous system glucose uptake (mmol/liter·min), EGP_{0-G} is endogenous glucose production extrapolated to zero plasma glucose concentration (mmol/liter·min), p_G is glucose effectiveness (min^{-1}), S_I is insulin sensitivity (liter/min·mU), $Q(t)$ is interstitial (effective) insulin concentration (mU/liter), $RGC(t)$ is renal glucose clearance (mmol/liter·min), and $P(t)$ is meal plasma glucose rate of appearance (mmol/liter·min).

This glucose model differs mathematically from the model developed by Chase *et al.*¹⁴ and Wong *et al.*¹⁵ in removal of insulin effect saturation and addition of the renal glucose clearance rate, $RGC(t)$. These two studies were done on highly dynamic, critically ill patients with high effective insulin resistance who were treated with intravenous insulin doses. Removal of the insulin effect saturation was deemed suitable for modeling more compliant, insulin-sensitive and stable type 1 diabetes patients treated with subcutaneously administered insulin.

$$RGC(t) = \begin{cases} \frac{GFR}{V_p m_b} (G(t) - RGT) & \text{if } G(t) > RGT \\ 0 & \text{if } G(t) \leq RGT \end{cases} \quad (2)$$

where $RGC(t)$ is renal glucose clearance (mmol/liter·min), GFR is glomerular filtration rate (liter/min), $G(t)$ is plasma glucose concentration (mmol/liter), RGT is renal glucose threshold (mmol/liter), V_p is glucose distribution volume (liter/kg), and m_b is body mass (kg).

Referring to **Equation (2)**, the renal glucose clearance rate, $RGC(t)$, models glucose removal by the kidney above the renal glucose threshold, RGT , using a linear relationship proportional to the glucose concentration above RGT and the glomerular filtration rate, GFR . From the study by Johansen and colleagues,¹⁶ this linear approximation is acceptable. Linear models have also been used in AIDA¹⁷ by Lehmann *et al.*¹⁸ and by Arleth *et al.*¹⁹

Insulin absorption from subcutaneous injection or infusion has been widely studied since Binder.²⁰ A novel, compartmental model of subcutaneous insulin absorption kinetics specifically developed for diabetes decision support has been presented.^{21,22} The model accounts for the volume and concentration dependence of regular human insulin absorption and models the absorption kinetics of six insulin types, including monomeric insulin and insulin glargine. Additionally, insulin injected or infused subcutaneously or intravenously can also be modeled. A schematic of the model adapted from Wong and colleagues²² is shown in **Figure 1**. This model is used in this study, which is the first application of the developed model in the control of type 1 diabetes.

Modeling of the meal glucose rate of appearance (R_a), including digestion, absorption, and transport of glucose, is a complex process not widely studied.²³ Meal carbohydrate amount and type are the main factors affecting meal glucose R_a or $P(t)$ in **Equations (1)** and **(6)**.^{24,25} However, clinical models of glucose R_a almost universally accept input of meal glucose amount only.^{18,26} *Glucose equivalent carbohydrate* introduced by Yates and Fletcher²³ to express carbohydrate values as monosaccharide equivalents necessarily depends on an a priori known content of the carbohydrate type within the meal to be consumed, which is typically unavailable. Carbohydrate counting is a technique^{27–29} commonly taught by diabetes care providers to improve glycemic management. Glycemic index, a measure of the effect of carbohydrate type, is not easily calculable for mixed meals³⁰ nor as readily available as carbohydrate content.

The minimal models of meal glucose R_a by Worthington³¹ and Lehmann *et al.*^{17,18} form the basis of the model used in this study. Referring to **Figure 2** and **Equations (3)–(5)**, the model consists of two compartments for the stomach and gut, with linear gastric emptying and gut-absorption rates to describe the plasma glucose R_a in **Equation (6)**. Another simplification is the expression of meal carbohydrate content (in grams) as equivalent to the same mass of glucose monosaccharide regardless of the meal carbohydrate type.²³ Again, such meal data are typically unavailable in a clinical setting. As such, the complex digestion processes, such as the hydrolysis of polysaccharides, are assumed linear and lumped into the simplified processes given earlier.

$$\frac{dSTO(t)}{dt} = -k_6 STO(t) + u_{CHO}(t) \quad (3)$$

$$\frac{dGUT(t)}{dt} = GABS(t) + k_6 STO(t) \quad (4)$$

$$GABS(t) = -\min(k_7 GUT(t), GABS_{\max}) \quad (5)$$

$$P(t) = \frac{GABS(t)}{0.18(V_p m_b)} \quad (6)$$

where $STO(t)$ is mass of carbohydrate/glucose in the stomach (g), $GUT(t)$ is mass of carbohydrate/glucose in the gut (g), $GABS$ is gut carbohydrate/glucose absorption rate (g/min), $GABS_{\max}$ is maximum gut carbohydrate/glucose absorption rate (g/min), k_6 is carbohydrate/glucose gastric emptying rate (min^{-1}), k_7 is carbohydrate/glucose gut-absorption rate (min^{-1}), $u_{CHO}(t)$ is meal carbohydrate/glucose input (g/min), $P(t)$ is meal plasma glucose rate of appearance (mmol/liter·min), V_p is glucose plasma distribution volume (liter/kg), and m_b is body mass (kg).

Worthington³¹ found that the one-compartment model with time delay had the smallest fitting error. However, this result was obtained with a model fit to plasma glucose data and is dependent on the model of glucose kinetics used. Lehmann and colleagues¹⁸ used a “complex” function to describe the gastric emptying rate from the stomach compartment. This study used a linear transport rate, k_6 , while the glucose input into the stomach compartment, $u_{CHO}(t)$, is described by a delta function. Similar to the saturable gastric emptying rate of Lehmann *et al.*,¹⁸ this study incorporated a saturable gut-absorption rate, $GABS_{\max}$. Saturable gut absorption has been postulated by Korach-Andre and colleagues³² in experiments using relatively large starch meals. However, this difference is likely to be small considering the minimal nature of both models. Referring to **Figure 3**, the effective gut-absorption rate is shown as a function

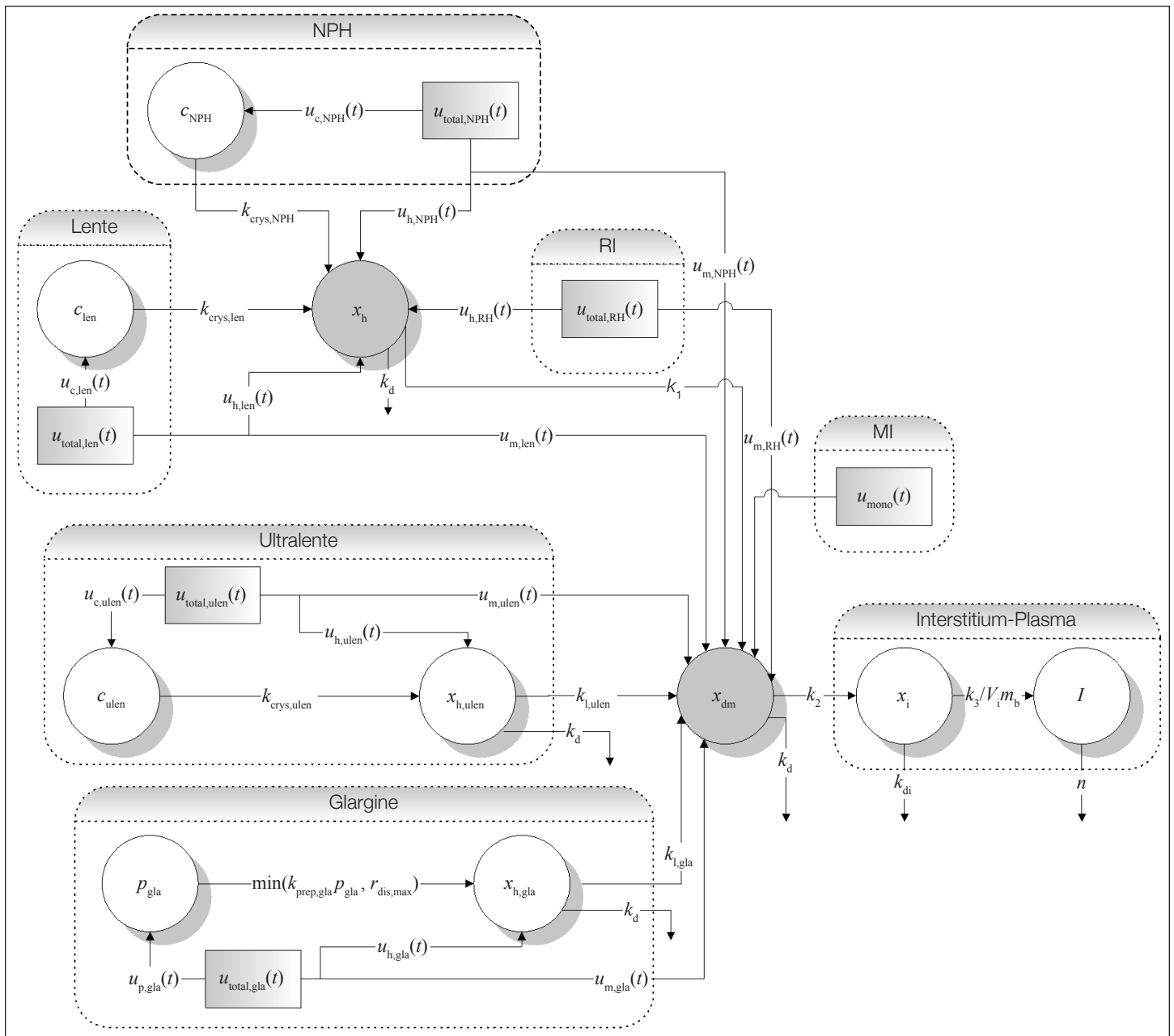


Figure 1. Structure of the subcutaneous insulin absorption kinetic model. The model is characterized by a common hexameric state compartment for regular insulin (RI), neutral protamine Hagedorn (NPH) insulin, and lente insulin (x_h), whereas those for insulins glargine and ultralente ($x_{h,ulen}$ and $x_{h,gla}$) are separate. A crystalline state compartment for NPH (c_{NPH}), lente (c_{len}), and ultralente (c_{ulen}) insulins and a precipitate compartment for insulin glargine (p_{gla}) model these protraction mechanisms. All insulin flows through a common dimeric–monomeric state compartment (x_{dm}), interstitium compartment (x_i), and finally into the plasma (I). Adapted from Wong *et al.*²²

of the mass of carbohydrate/glucose in the GUT compartment. Addition of the saturable term $GABS_{max}$ effectively makes the gut absorption rate nonlinear as a function of the amount of carbohydrate in the gut. This dynamic is similar to that of the nonlinear three-compartment model of Dalla Man *et al.*,²⁶ which consists of dual stomach compartments with a nonlinear gastric emptying rate with four identified parameters. The nonlinear gastric emptying term is described by a

hyperbolic tangent function as a function of the *proportion* of the consumed carbohydrate remaining in the stomach. There is no saturation term considered for large, absolute meals.

Referring to **Table 1**, the values of patient-independent model population constants are a priori identified from literature. The renal glucose threshold, RGT , has been shown to vary considerably in type 1 diabetes,¹⁶

but median values of 10 mmol/liter have been widely reported. The glucose distribution volume, V_p , is taken to be 0.22 liter/kg, the same value used by Lehmann *et al.*¹⁸ The glomerular filtration rate, GFR , is taken as 0.12 liter/min or 120 ml/min, which reflects the average adult GFR of 125 ml/min.³³

In a study by Dalla Man *et al.*,³⁴ the maximum meal R_a ($R_{a\text{ meal}}$) was $\sim 8\text{--}9$ mg/kg-min after an oral dose of 1 g/kg glucose. In the study by Korach-Andre *et al.*,³² the exogenous meal R_a ($R_{a\text{ exo}}$) was approximately 7–9 mg/kg-min for a meal of 4 g/kg of starch (~ 4.4 g/kg glucose). Despite

the fourfold increase in glucose load, the maximum R_a remains at ~ 9 mg/kg-min or ~ 0.72 g/min for an average adult. In a study by Noah *et al.*,³⁵ a higher figure still of 11 mg/kg-min was reported in a porcine model. The *maximum* value of the rate of gut absorption is taken as 1.1 g/min using the Noah *et al.*³⁵ study as a basis, assuming a 100-kg body weight.

The proportion of glucose lost to first-pass splanchnic uptake is still being debated, with proportions from negligible^{36,37} to as high as 30% reported in some studies.³⁸ As there will be no tracer data in the intended application of the model, negligible losses from first-pass splanchnic sequestration and complete absorption are assumed for simplicity³⁹ with complete absorption of meal glucose. The values of k_6 and k_7 are optimized using nonlinear least squares to model-independent, mixed-meal tracer glucose R_a data³⁴ (results not shown).

The values of CNS , EGP_{0-G} , and p_G are derived from results of studies done by Del Prato *et al.*^{40,41} Like the minimal model of Bergman and colleagues,⁴² the model is unable to differentiate noninsulin-mediated glucose uptake from production, which is lumped into a linear relationship with glucose. Referring to **Figures 4** and **5**, total body glucose uptake (TBGU) and hepatic glucose production (HGP) data described elsewhere^{40,41} are used to identify CNS , EGP_{0-G} , and p_G . Data at glucose exceeding the approximate RGT of 10 mmol/liter are ignored to eliminate the need to evaluate renal glucose clearance, RGC , and associated errors. Under fasting and insulinopenic conditions, the $P(t)$ and $S_7G(t)Q(t)$ terms of **Equation (1)** can be further eliminated. By the linear

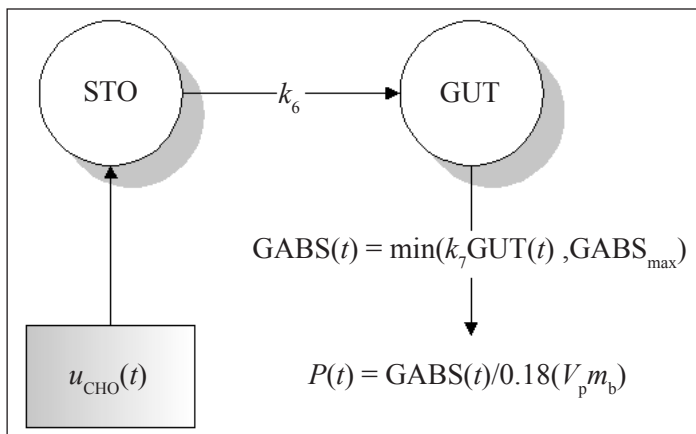


Figure 2. Structure of the meal glucose rate of the appearance model. The model is characterized by a delta function to describe meal glucose input [$u_{CHO}(t)$], linear gastric emptying (k_6), and gut absorption (k_7) rates and saturable gut absorption ($GABS_{max}$).

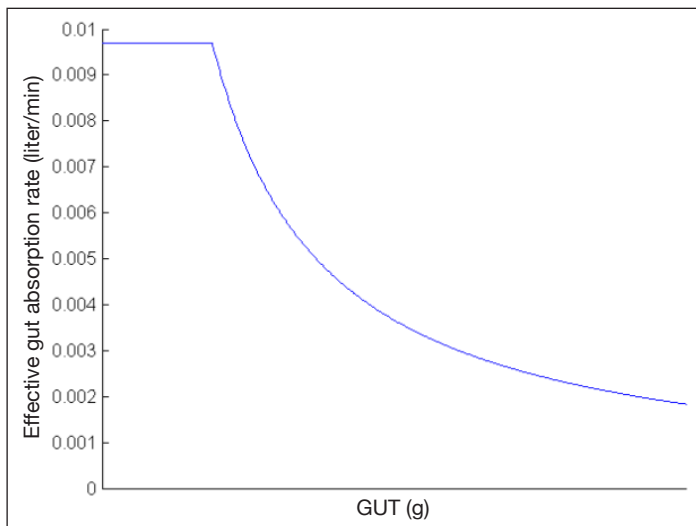


Figure 3. Qualitative plot of the *effective* gut absorption rate as a function of the mass of carbohydrate/glucose in the *GUT* compartment. While the process of gastric emptying is linear, addition of the saturable gut absorption term, $GABS_{max}$, of 1.1 g/min effectively makes the process of gut absorption, and hence meal glucose R_a , nonlinear. At low glucose levels in the gut, the effective gut absorption rate is 0.0097 liter/min.

Table 1. A Priori Identified Model Constants Obtained from the Literature Except Linear Gastric Emptying and Gut Absorption Rates (k_6 and k_7 , Respectively), Which Were Optimized Using Nonlinear Least Squares to Model-Independent, Mixed-Meal Tracer Glucose R_a Data³⁴

Model constants	Values (units)
$GABS_{max}$	1.1 (g/min)
p_G	0.0060 (min^{-1})
CNS	1.7 (mg/kg-min)
EGP_{0-G}	3.0 (mg/kg-min)
GFR	0.12 (liter/min)
RGT	10 (mmol/liter)
V_p	0.22 (liter/kg)
k_6	0.0388 (min^{-1})
k_7	0.0097 (min^{-1})

definition of the effect of hyperglycemia on TBGU, *CNS* can then be derived as the “virtual” *y* intercept of the linear TBGU curve. The term “virtual” is used, as no glucose uptake is theoretically possible at zero glucose. The central nervous system glucose uptake *CNS* is saturated at 3.3 mmol/liter and is relatively insensitive to insulin and glucose.^{43,44} At euglycemia, *CNS* accounts for ~70% of all noninsulin-mediated glucose uptake,⁴⁵ and this proportion is likely to increase with hypoglycemia. Hence, use of the term *CNS* for the virtual *y* intercept of the linear TBGU curve is justified.

Similarly, by the linear definition of the effect of hyperglycemia on HGP, EGP_{0-G} is the *y* intercept of the linear HGP curve and p_G is the slope of the combined TBGU and HGP curve. Hence, p_G is similar to the minimal model glucose effectiveness, S_G , but is defined under conditions of insulinopenia or subbasal insulin rather than basal insulin.⁴⁶

Unlike the minimal model, the insulin model in this study models the absolute insulin concentration, not insulin concentration above basal. In type 1 diabetes, conditions of basal insulin are not necessarily met all the time. Using data from Del Prato and colleagues⁴¹ for an insulinopenic normal cohort (Figure 4), values of $CNS = 1.4$ mg/kg·min, $EGP_{0-G} = 2.6$ mg/kg·min, and $p_G = 0.006$ min⁻¹ are obtained compared to $CNS = 1.3$ mg/kg·min, $EGP_{0-G} = 3.0$ mg/kg·min, and $p_G = 0.009$ min⁻¹ under basal insulin conditions

(figure not shown). Compared to insulinopenia, the presence of basal insulin results in overestimation of p_G , although this value is still approximately half that of published values of the minimal model S_G for a normal cohort ~0.024 min⁻¹.⁴⁶

Using data of Del Prato *et al.*⁴⁰ for an insulin-dependent diabetes mellitus (IDDM) cohort under basal insulin (Figure 5), values of $CNS = 1.7$ mg/kg·min, $EGP_{0-G} = 3.0$ mg/kg·min, and $p_G = 0.006$ min⁻¹ were obtained. Hence, p_G of the normal, insulinopenic cohort⁴¹ is similar to the IDDM cohort under basal insulin.⁴⁰ This result is logical, as S_G is decreased in IDDM,⁴⁶ whereas basal insulin increases S_G , either by increased glucose uptake⁴⁴ or by suppression of endogenous glucose production.⁴¹ In IDDM, the p_G obtained is also approximately half that of published S_G values of ~0.013 min⁻¹.⁴⁶ One explanation is the elimination of data at high glucose concentrations from the p_G analysis, which, if unaccounted for, would include the effect of urinary glucose excretion, thereby increasing the “effective” glucose uptake. From this investigation, it can be deduced that for an IDDM cohort under conditions of insulinopenia, p_G must have an upper bound of 0.006 min⁻¹, which is assumed in this study. The values of *CNS* obtained are in agreement with other results,^{45,47,48} and the assumption that *CNS* is approximately equal to the virtual *y* intercept of the linear TBGU curve is valid. A summary of the values of the model constants is shown in Table 1.

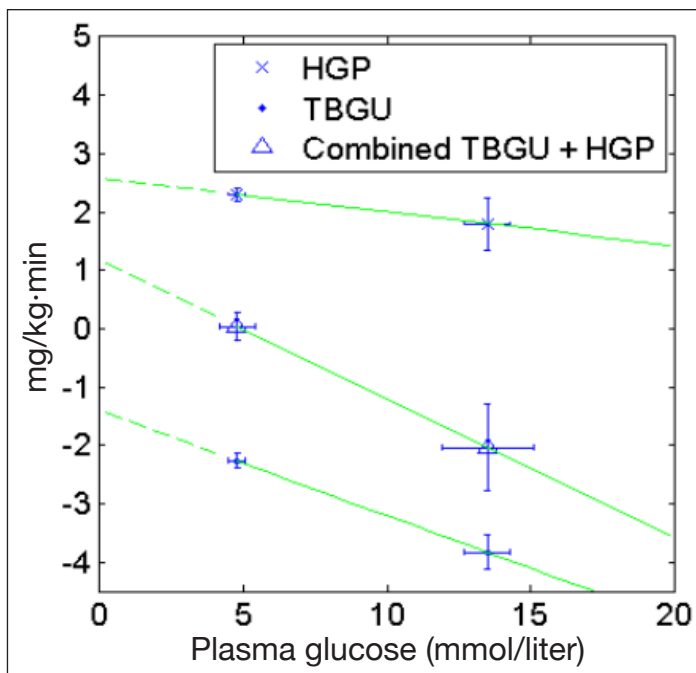


Figure 4. Using HGP and TBGU data from Del Prato and colleagues⁴¹ for an insulinopenic normal cohort, values of $CNS = 1.4$ mg/kg·min, $EGP_{0-G} = 2.6$ mg/kg·min, and $p_G = 0.006$ min⁻¹ can be calculated by linear regression.

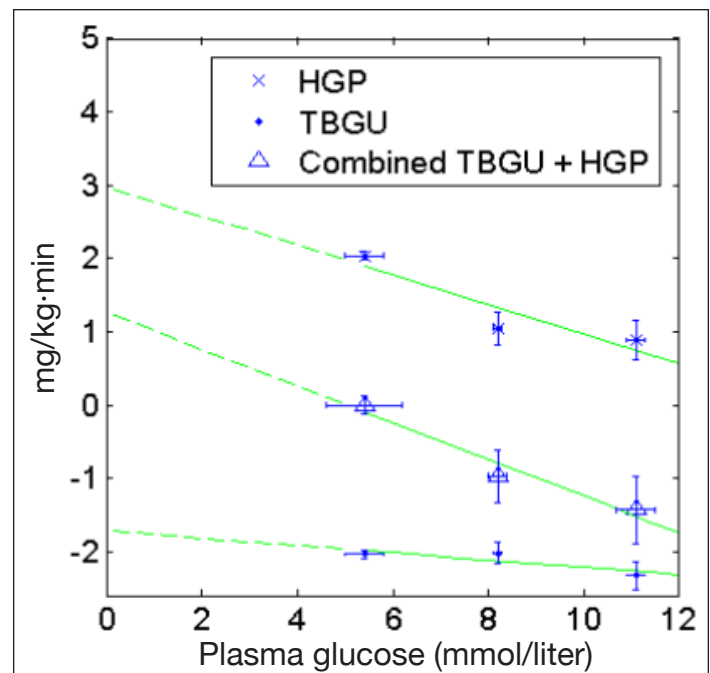


Figure 5. Using HGP and TBGU data of Del Prato and colleagues⁴⁰ for an IDDM cohort under basal insulin, values of $CNS = 1.7$ mg/kg·min, $EGP_{0-G} = 3.0$ mg/kg·min, and $p_G = 0.006$ min⁻¹ can be calculated by linear regression.

Methods

Patient Cohort

Patient data used in this study were obtained from AIDA on-line², the Web-based version of the AIDA educational diabetes program.⁴⁹ AIDA on-line² incorporates the physiological model developed by Lehmann *et al.*¹⁸ and can simulate glycemic levels for any insulin or meal stimuli over a period of 1 day. Patient data ($n = 40$) for this study were obtained from sample diabetes case scenarios available with AIDA on-line². Referring to **Table 2**, each patient case is unique in body weight, meals/carbohydrates consumed, and insulin treatment. Each patient also has unique clinical variables of hepatic and peripheral insulin sensitivity, glucose renal threshold, and glomerular filtration rate. Hence, the AIDA on-line² cohort represents a broad range of patients and possible clinical behavior. To retrieve blood glucose, plasma insulin, and meal glucose absorption rates from AIDA on-line², the “Advanced” display is selected to output data in text format. A sample of these data is shown in **Figure 6**.

Simulation Method

For *in silico* simulation, the virtual patient method is used.^{50,51} This method has been utilized to develop effective glycemic control protocols by simulating the physiological glycemic response to glucose and insulin stimuli.^{50–52} The glycemic responses are generated with patient-specific $S_i(t)$ profiles derived from retrospective data. This clinically validated method⁵⁰ enables extensive simulations to be performed in a short time for rapid development and testing of any control methodology.

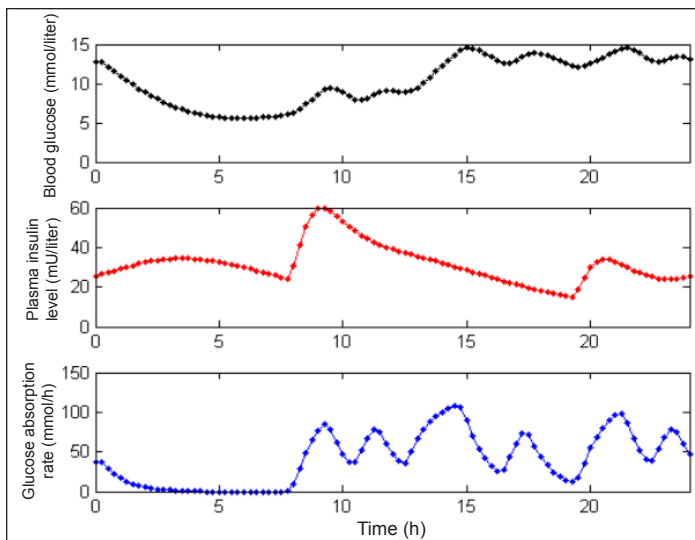


Figure 6. Sample raw blood glucose, plasma insulin level, and glucose absorption rate data from AIDA on-line².⁴⁹

In silico simulation was performed using MATLAB[®] (The Mathworks, Natick, MA) implemented on a personal computer notebook (Pentium M 1.7 GHz).

To obtain the retrospective $S_i(t)$ patient data profiles, the model is first fitted to data using the linear and convex, integral-based parameter identification method.⁵³

Equation (1) can be expressed in a generic integral form [**Equation (7)**] for period t_{i-1} to t_i , which can then be rearranged into a set of linear equations as shown in **Equation (9)**. All quantities in **Equation (7)** are modeled and, as such, are known except for $G(t)$.

$$\begin{aligned} \int_{t_{i-1}}^{t_i} \dot{G}(t)dt &= \int_{t_{i-1}}^{t_i} [EGP_{0-G} - p_G G(t) - \bar{S}_{t,i} G(t)Q(t) - RGC(t) - CNS + P(t)]dt \\ G(t_i) - G(t_{i-1}) &= \int_{t_{i-1}}^{t_i} [EGP_{0-G} - RGC(t) - CNS + P(t)]dt \\ &\quad - p_G \int_{t_{i-1}}^{t_i} G(t)dt \\ &\quad - \bar{S}_{t,i} \int_{t_{i-1}}^{t_i} G(t)Q(t)dt \\ \bar{S}_{t,i} \int_{t_{i-1}}^{t_i} G(t)Q(t)dt &= \int_{t_{i-1}}^{t_i} [EGP_{0-G} - RGC(t) - CNS + P(t)]dt \\ &\quad - p_G \int_{t_{i-1}}^{t_i} G(t)dt \\ &\quad - [G(t_i) - G(t_{i-1})] \end{aligned} \quad (7)$$

$$G(t) = \sum_{i=1}^N \left[\bar{G}_{i-1} + (\bar{G}_i - \bar{G}_{i-1}) \left(\frac{t - t_{i-1}}{t_i - t_{i-1}} \right) \right] (H(t - t_{i-1}) - H(t - t_i)) \quad (8)$$

AIDA on-line² uses a first-order Euler integration method with a 15-minute step size to solve the plasma glucose model equation.⁵⁴ To determine $G(t)$ to solve **Equation (7)**, AIDA on-line² glucose data are interpolated linearly to obtain a piecewise linear $G(t)$ function [**Equation (8)**].

The $t_i - t_{i-1}$ time interval for the optimization of $S_i(t)$ is chosen arbitrarily as 10 minutes. **Equation (8)** is solved using a proprietary MATLAB linear solver. Referring to **Figure 7** and **Equations (9)** and **(10)**, a stepwise, time-variant $S_i(t)$ with a 10-minute step interval is obtained.

$$\bar{A} \{ \bar{S}_{t,i} \} = b \quad (9)$$

where

$$\begin{aligned} \bar{A} &= \int_{t_{i-1}}^{t_i} G(t)Q(t)dt \\ \bar{b} &= \int_{t_{i-1}}^{t_i} [EGP_{0-G} - RGC(t) - CNS + P(t)]dt \\ &\quad - p_G \int_{t_{i-1}}^{t_i} G(t)dt \\ &\quad - [G(t_i) - G(t_{i-1})] \end{aligned}$$

$$S_i(t) = \sum_{i=1}^N \bar{S}_{t,i} (H(t - t_{i-1}) - H(t - t_i)) \quad (10)$$

Table 2.
Details of Patient Cohort ($n = 40$) from AIDA² On-line Showing Body Weight, Total Carbohydrate Consumed, Total Prandial Insulin Dose, Total Basal Insulin Dose, and Unique Clinical Variables of Hepatic and Peripheral Insulin Sensitivity, Glucose Renal Threshold, and Glomerular Filtration Rate

Case number	Body weight (kg)	Total carbohydrate consumed (g)	Total prandial insulin dose (U)	Total basal insulin dose (U)	Renal threshold	Renal function	Hepatic insulin sensitivity	Peripheral insulin sensitivity
1	70	130	7	30	Normal	Normal	Reduced	Reduced
2	68	180	13	10	High	Normal	Increased	Increased
3	70	120	9	13	Normal	Normal	Normal	Increased
4	60	180	13	12	Normal	Normal	Increased	Increased
5	98	180	12	12	Normal	Normal	Normal	Normal
6	76	120	8	28	Normal	Normal	Reduced	Increased
7	70	90	7	24	Normal	Normal	Increased	Reduced
8	70	120	10	20	Normal	Normal	Reduced	Increased
9	70	180	12	12	High	Normal	Normal	Increased
10	70	120	15	8	Normal	Normal	Normal	Increased
11	70	205	16	22	Normal	Normal	Normal	Increased
12	70	185	24	20	Normal	Normal	Reduced	Increased
13	76	100	8	26	Normal	Normal	Normal	Increased
14	65	70	5	20	Normal	Normal	Reduced	Normal
15	99	115	6	42	Normal	Normal	Reduced	Normal
16	70	180	9	32	Normal	Normal	Reduced	Increased
17	70	110	10	24	Normal	Normal	Reduced	Increased
18	60	165	18	36	High	Normal	Reduced	Increased
19	60	180	12	12	Normal	Normal	Normal	Increased
20	70	105	8	36	Normal	Normal	Normal	Increased
21	98	295	34	40	Normal	Normal	Reduced	Reduced
22	75	70	Biphasic 40		Normal	Normal	Reduced	Reduced
23	87	177	38	12	Normal	Normal	Reduced	Increased
24	76	95	7	24	Normal	Normal	Normal	Increased
25	70	120	18	28	Normal	Normal	Reduced	Normal
26	80	170	Biphasic 20		Normal	Normal	Normal	Increased
27	70	120	9	13	Low	Normal	Normal	Normal
28	75	85	5	40	Normal	Normal	Normal	Increased
29	83	60	12	25	Normal	Normal	Reduced	Normal
30	80	165	16	36	Normal	Normal	Reduced	Increased
31	99	220	29	14	Low	Normal	Normal	Increased
32	90	70	0	28	Normal	Normal	Reduced	Reduced
33	98	180	0	18	Normal	Normal	Normal	Increased
34	60	175	17	13	High	Normal	Normal	Increased
35	60	170	22	10	Normal	Normal	Normal	Increased
36	70	100	8	32	Normal	Normal	Reduced	Increased
37	70	105	9	36	High	Normal	Reduced	Reduced
38	70	95	Biphasic 26		Normal	Normal	Normal	Reduced
39	70	110	12	35	High	Normal	Reduced	Increased
40	76	100	7	30	Normal	Normal	Normal	Normal

A proprietary MATLAB numerical ODE solver is used to solve the model equations with a 1-minute time step. Biphasic insulin preparations are treated as in AIDA with the insulin response assumed to be a superposition of the individual components of the preparation.¹⁸ This is an acknowledged simplification considering the large variety and lack of data on such preparations.

The numerical solution to the model equations forms the *in silico* simulation tool. With the set of 40 virtual

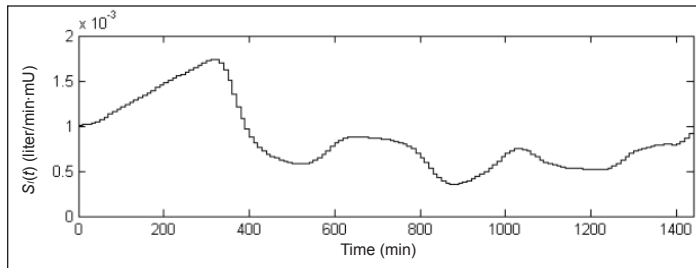


Figure 7. Sample patient $S_I(t)$ profile as obtained from model fit. Note the 10-minute interval for fitting the stepwise, time-variant $S_I(t)$.

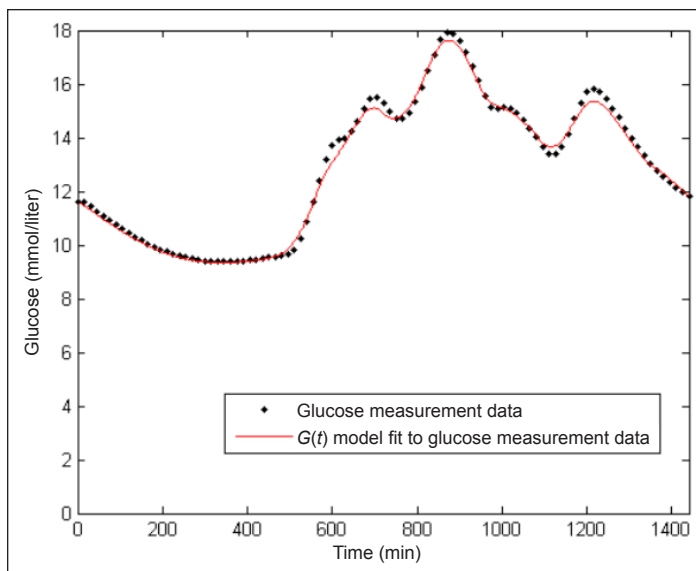


Figure 8. $G(t)$ model fit to glucose measurement data for Patient 1 shown with glucose measurement data from AIDA on-line².

patient $S_I(t)$ profiles, any meal or subcutaneous insulin input and its effect on glycemia can be simulated with the assumption that S_I is independent of the inputs administered, i.e., the virtual patient. This opens the possibility of simulating any glycemic control protocol, even current clinical methods.^{55–57} An initial validation would be to replicate long-term glycemic control outcomes, e.g., hemoglobin A1c.

Results

To gauge the model fit to data, absolute and absolute percentage errors of the $G(t)$ model fit to the AIDA on-line² patient data cohort are shown in **Tables 3** and **4**. In **Table 3**, per patient errors are shown, whereas total errors over the entire cohort are shown in **Table 4**. A sample $G(t)$ fit is also shown in **Figure 8**.

From **Table 3**, the per patient median (95% range) absolute percentage error in $G(t)$ is 1.24% (0.09–4.85%), which translates into a per patient absolute error in $G(t)$ of 0.11 mmol/liter (0.01–0.43 mmol/liter). Over the entire cohort the figures are 1.33% (0.08–7.20%) and 0.12 mmol/liter (0.01–0.56 mmol/liter), which are similar. The errors reported are extremely low and within the measurement errors of clinical methods of glucose measurement in current use. This shows that the model and S_I identification method is capable of capturing all patient $G(t)$ dynamics, which will produce a more physiologically accurate simulation.

Conclusions

An *in silico* simulation tool was presented that utilizes an extended model of glucose kinetics, a simple glucose rate of appearance model, and the novel application of a subcutaneous insulin pharmacokinetic model. Models are identified to a physiological cohort of type 1 diabetes virtual patients. To corroborate the approach initially, an *in silico* simulation with data from the patient cohort using the virtual patient simulation method is planned.

Table 4. Total Absolute and Absolute Percentage $G(t)$ Model Fit Errors to Patient Cohort Data ($n = 40$) from AIDA On-line²

Absolute % $G(t)$ fit error			Absolute $G(t)$ fit error (mmol/liter)		
Median	5th percentile	95th percentile	Median	5th percentile	95th percentile
1.33	0.08	7.20	0.12	0.01	0.56

Table 3.
Per Patient Absolute and Absolute Percentage $G(t)$ Model Fit Errors to Patient Cohort Data ($n = 40$) from AIDA On-line²

Case number	Absolute % $G(t)$ fit error			Absolute $G(t)$ fit error (mmol/liter)		
	Median	5th percentile	95th percentile	Median	5th percentile	95th percentile
1	0.84	0.08	2.87	0.10	0.01	0.43
2	1.28	0.05	7.14	0.10	0.00	0.50
3	1.19	0.02	3.56	0.12	0.00	0.37
4	1.72	0.05	7.84	0.12	0.00	0.42
5	0.94	0.11	3.24	0.11	0.01	0.36
6	1.25	0.04	4.89	0.13	0.00	0.53
7	1.93	0.11	4.52	0.07	0.00	0.20
8	0.96	0.05	4.46	0.09	0.00	0.49
9	1.03	0.10	2.94	0.12	0.01	0.39
10	1.92	0.28	4.27	0.17	0.02	0.39
11	3.09	0.20	14.04	0.20	0.01	2.39
12	1.23	0.05	8.78	0.13	0.00	0.70
13	1.08	0.09	4.80	0.07	0.00	0.26
14	0.47	0.04	3.43	0.05	0.00	0.47
15	1.00	0.12	3.84	0.08	0.01	0.29
16	1.61	0.11	5.84	0.18	0.01	0.59
17	1.31	0.06	4.38	0.13	0.00	0.38
18	3.34	0.32	7.84	0.21	0.03	0.80
19	1.23	0.09	4.14	0.16	0.01	0.52
20	2.89	0.17	21.39	0.13	0.00	0.89
21	2.73	0.49	7.17	0.32	0.06	0.93
22	0.88	0.11	3.95	0.09	0.01	0.50
23	1.50	0.03	4.96	0.11	0.00	0.33
24	1.98	0.21	6.67	0.14	0.01	0.43
25	1.37	0.02	7.44	0.09	0.00	0.59
26	0.67	0.09	2.48	0.07	0.01	0.31
27	0.69	0.08	2.74	0.06	0.01	0.27
28	0.81	0.09	6.27	0.05	0.00	0.36
29	0.81	0.15	4.48	0.07	0.01	0.40
30	9.36	0.98	37.10	0.72	0.06	2.56
31	1.16	0.11	8.67	0.08	0.01	0.44
32	0.60	0.06	2.36	0.06	0.01	0.28
33	0.93	0.13	2.72	0.10	0.01	0.29
34	1.84	0.01	5.93	0.15	0.00	0.44
35	3.30	0.18	11.70	0.26	0.01	1.06
36	1.36	0.19	5.05	0.12	0.01	0.39
37	0.94	0.03	3.38	0.12	0.00	0.46
38	0.73	0.08	3.07	0.08	0.01	0.40
39	1.29	0.04	5.53	0.11	0.00	0.51
40	1.70	0.20	7.20	0.10	0.01	0.31
Median	1.24	0.09	4.85	0.11	0.01	0.43
Range	0.47–9.36	0.01–0.98	2.36–37.10	0.05–0.72	0.00–0.06	0.20–2.56

Funding:

Financial support was received from the Tertiary Education Commission Te Amorangi Matauranga Matua Bright Futures Top Achiever Doctoral Scholarship.

Acknowledgements:

The authors acknowledge Dr. Eldon Lehmann and AIDA on-line² for the use of patient data in this study.

References:

1. Bequette BW. A critical assessment of algorithms and challenges in the development of a closed-loop artificial pancreas. *Diabetes Technol Ther.* 2005;7(1):28-47.
2. Bellazzi R, Nucci G, Cobelli C. The subcutaneous route to insulin-dependent diabetes therapy. *IEEE Eng Med Biol Mag.* 2001;20(1):54-64.
3. Steil GM, Rebrin K, Darwin C, Hariri F, Saad MF. Feasibility of automating insulin delivery for the treatment of type 1 diabetes. *Diabetes.* 2006;55(12):3344-50.
4. Steil GM, Panteleon AE, Rebrin K. Closed-loop insulin delivery--the path to physiological glucose control. *Adv Drug Deliv Rev.* 2004;56(2):125-44.
5. Klonoff DC. Continuous glucose monitoring: roadmap for 21st century diabetes therapy. *Diabetes Care.* 2005;28(5):1231-9.
6. Guidance on the use of continuous subcutaneous insulin infusion for diabetes. Technology Appraisal Guidance No. 57, National Institute for Clinical Excellence; 2003. Available from: www.nice.org.uk.
7. Position statement on insulin pump therapy. Position statement on insulin pump therapy, Diabetes UK [cited 2007 Aug 8]. Available from: www.diabetes.org.uk.
8. ADA. Standards of medical care in diabetes-2006. *Diabetes Care.* 2006;29; S4-S42.
9. Mainous AG 3rd, Diaz VA, Saxena S, Baker R, Everett CJ, Koopman RJ, Majeed A. Diabetes management in the USA and England: comparative analysis of national surveys. *J R Soc Med.* 2006;99(9):463-9.
10. Cohen M, Boyle E, Delaney C, Shaw J. A comparison of blood glucose meters in Australia. *Diabetes Res Clin Pract.* 2006;71(2):113-8.
11. Guerci B, Floriot M, Böhme P, Durain D, Benichou M, Jellimann S, Drouin P. Clinical performance of CGMS in type 1 diabetic patients treated by continuous subcutaneous insulin infusion using insulin analogs. *Diabetes Care.* 2003;26(3):582-9.
12. Gerich JE. Novel insulins: Expanding options in diabetes management. *Am J Med.* 2002;113(4):308-16.
13. Wong J, Chase JG, Hann CE, Lotz TF, Lin J, Le Compte A, Shaw GM. Monte Carlo analysis of an adaptive protocol for the clinical control of type 1 diabetes. *Diabetes Sci Technol.* 2008;2(3): in preparation.
14. Chase JG, Shaw GM, Lin J, Doran CV, Hann C, Robertson MB, Browne PM, Lotz T, Wake GC, Broughton B. Adaptive bolus-based targeted glucose regulation of hyperglycaemia in critical care. *Med Eng Phys.* 2005;27(1):1-11.
15. Wong XW, Singh-Levett I, Hollingsworth LJ, Shaw GM, Hann CE, Lotz T, Lin J, Wong OS, Chase JG. A novel, model-based insulin and nutrition delivery controller for glycemic regulation in critically ill patients. *Diabetes Technol Ther.* 2006;8(2):174-90.
16. Johansen K, Svendsen PA, Lørup B. Variations in renal threshold for glucose in Type 1 (insulin-dependent) diabetes-mellitus. *Diabetologia.* 1984;26(3):180-2.
17. Lehmann ED, Deutsch T, Carson ER, Sönksen PH. Aida: an interactive diabetes adviser. *Comput Methods Programs Biomed.* 1994;41(3-4):183-203.
18. Lehmann ED, Deutsch T. A physiological model of glucose-insulin interaction in type 1 diabetes mellitus. *J Biomed Eng.* 1992;14(3):235-42.
19. Arleth T, Andreassen S, Federici MO, Benedetti MM. A model of the endogenous glucose balance incorporating the characteristics of glucose transporters. *Comput Methods Programs Biomed.* 2000;62(3):219-34.
20. Binder C. Absorption of injected insulin. A clinical-pharmacological study. *Acta Pharmacol Toxicol (Copenh).* 1969;27 Suppl 2:1-84.
21. Wong J, Chase JG, Hann CE, Shaw GM, Lotz TF, Lin J, Le Compte AJ. A subcutaneous insulin pharmacokinetic model for computer simulation in a diabetes decision support role: validation and simulation. *J Diabetes Sci Technol.* In press 2008.
22. Wong J, Chase JG, Hann CE, Shaw GM, Lotz TF, Lin J, Le Compte AJ. A subcutaneous insulin pharmacokinetic model for computer simulation in a diabetes decision support role: model structure and parameter identification. *J Diabetes Sci Technol.* In press 2008.
23. Yates TL, Fletcher LR. Prediction of a glucose appearance function from foods using deconvolution. *Ima J Math Appl Med Biol.* 2000;17(2):169-84.
24. Wolever TM, Bolognesi C. Source and amount of carbohydrate affect postprandial glucose and insulin in normal subjects. *J Nutr.* 1996;126(11):2798-806.
25. Wolever TM, Bolognesi C. Prediction of glucose and insulin responses of normal subjects after consuming mixed meals varying in energy, protein, fat, carbohydrate and glycemic index. *J Nutr.* 1996;126(11):2807-12.
26. Dalla Man C, Camilleri M, Cobelli C. A system model of oral glucose absorption: validation on gold standard data. *IEEE Trans Biomed Eng.* 2006;53(12 Pt 1):2472-8.
27. Bruttomesso D, Pianta A, Crazzolara D, Capparotto C, Dainese E, Zurlo C, Minicuci N, Briani G, Tiengo A. Teaching and training programme on carbohydrate counting in Type 1 diabetic patients. *Diabetes Nutr Metab.* 2001;14(5):259-67.
28. Warshaw HS, Kulkarni K. Complete guide to carb counting: how to take the mystery out of carb counting and unlock the secrets to blood glucose control. 2nd ed. Virginia: American Diabetes Association; 2004.
29. Gregory RP, Davis DL. Use of carbohydrate counting for meal planning in type I diabetes. *Diabetes Educ.* 1994;20(5):406-9.
30. Flint A, Møller BK, Raben A, Pedersen D, Tetens I, Holst JJ, Astrup A. The use of glycaemic index tables to predict glycaemic index of composite breakfast meals. *Br J Nutr.* 2004;91(6):979-89.
31. Worthington DR. Minimal model of food absorption in the gut. *Med Inform (Lond).* 1997;22(1):35-45.
32. Korach-André M, Roth H, Barnoud D, Péan M, Péronnet F, Leverve X. Glucose appearance in the peripheral circulation and liver glucose output in men after a large 13C starch meal. *Am J Clin Nutr.* 2004;80(4):881-6.
33. Guyton AC, Hall JE. Textbook of medical physiology. 10th ed. London: Saunders; 2000.

34. Dalla Man C, Caumo A, Basu R, Rizza R, Toffolo G, Cobelli C. Minimal model estimation of glucose absorption and insulin sensitivity from oral test: validation with a tracer method. *Am J Physiol Endocrinol Metab.* 2004;287(4):E637-43.
35. Noah L, Krempf M, Lecannu G, Maugère P, Champ M. Bioavailability of starch and postprandial changes in splanchnic glucose metabolism in pigs. *Am J Physiol Endocrinol Metab.* 2000;278(2):E181-8.
36. Mari A, Wahren J, DeFronzo RA, Ferrannini E. Glucose absorption and production following oral glucose: comparison of compartmental and arteriovenous-difference methods. *Metabolism* 1994;43(11):1419-25.
37. Ferrannini E, Bjorkman O, Reichard GA Jr, Pilo A, Olsson M, Wahren J, DeFronzo RA. The disposal of an oral glucose load in healthy subjects. A quantitative study. *Diabetes.* 1985;34(6):580-8.
38. Capaldo B, Gastaldelli A, Antonello S, Auletta M, Pardo F, Ciociaro D, Guida R, Ferrannini E, Saccà L. Splanchnic and leg substrate exchange after ingestion of a natural mixed meal in humans. *Diabetes.* 1999;48(5):958-66.
39. Livesey G, Wilson PD, Dainty JR, Brown JC, Faulks RM, Roe MA, Newman TA, Eagles J, Mellon FA, Greenwood RH. Simultaneous time-varying systemic appearance of oral and hepatic glucose in adults monitored with stable isotopes. *Am J Physiol.* 1998;275(4 Pt 1):E717-28.
40. Del Prato S, Matsuda M, Simonson DC, Groop LC, Sheehan P, Leonetti F, Bonadonna RC, DeFronzo RA. Studies on the mass action effect of glucose in NIDDM and IDDM: evidence for glucose resistance. *Diabetologia.* 1997;40(6):687-97.
41. Del Prato S, Riccio A, Vigili de Kreutzenberg S, Dorella M, Tiengo A, DeFronzo RA. Basal plasma insulin levels exert a qualitative but not quantitative effect on glucose-mediated glucose uptake. *Am J Physiol.* 1995;268(6 Pt 1):E1089-95.
42. Bergman RN, Ider YZ, Bowden CR, Cobelli C. Quantitative estimation of insulin sensitivity. *Am J Physiol.* 1979;236(6):E667-77.
43. Siesjö BK. Hypoglycemia, brain metabolism, and brain damage. *Diabetes Metab Rev.* 1988;4(2):113-44.
44. Best JD, Taborsky GJ Jr, Halter JB, Porte D Jr. Glucose disposal is not proportional to plasma glucose level in man. *Diabetes.* 1981;30(10):847-50.
45. Baron AD, Brechtel G, Wallace P, Edelman SV. Rates and tissue sites of non-insulin- and insulin-mediated glucose uptake in humans. *Am J Physiol.* 1988;255(6 Pt 1):E769-74.
46. Best JD, Kahn SE, Ader M, Watanabe RM, Ni TC, Bergman RN. Role of glucose effectiveness in the determination of glucose tolerance. *Diabetes Care.* 1996;19(9):1018-30.
47. Scheinberg P. Observations on cerebral carbohydrate metabolism in man. *Ann Intern Med.* 1965;62:367-71.
48. Boyle PJ, Scott JC, Krentz AJ, Nagy RJ, Comstock E, Hoffman C. Diminished brain glucose metabolism is a significant determinant for falling rates of systemic glucose utilization during sleep in normal humans. *J Clin Invest.* 1994;93(2):529-35.
49. Reed K, Lehmann ED. Diabetes website review: www.2aida.org. *Diabetes Technol Ther.* 2005;7(5):741-54.
50. Chase JG, Shaw GM, Lotz T, LeCompte A, Wong J, Lin J, Lonergan T, Willacy M, Hann CE. Model-based insulin and nutrition administration for tight glycaemic control in critical care. *Curr Drug Deliv.* 2007;4(4):283-96.
51. Chase JG, Wong XW, Singh-Levett I, Hollingsworth LJ, Hann CE, Shaw GM, Lotz T, Lin J. Simulation and initial proof-of-concept validation of a glycaemic regulation algorithm in critical care. *Control Eng Pract.* In press 2008.
52. Lonergan T, Le Compte A, Willacy M, Chase JG, Shaw GM, Wong XW, Lotz T, Lin J, Hann CE. A simple insulin-nutrition protocol for tight glycemic control in critical illness: development and protocol comparison. *Diabetes Technol Ther.* 2006;8(2):191-206.
53. Hann CE, Chase JG, Lin J, Lotz T, Doran CV, Shaw GM. Integral-based parameter identification for long-term dynamic verification of a glucose-insulin system model. *Comput Methods Programs Biomed.* 2005;77(3):259-70.
54. Lehmann ED, Deutsch T. AIDA2: a Mk. II automated insulin dosage advisor. *J Biomed Eng.* 1993;15(3):201-11.
55. BD Diabetes Learning Centre. Insulin therapies. Managing diabetes with insulin. 2006. Available from: <http://www.bddiabetes.com/us/main.aspx?cat=1&id=151>.
56. Walsh J, Roberts R. The pocket pancreas: your diabetes guide for improved blood sugars. Diabetes Services Inc.; 1994.
57. Hanas R. Type 1 diabetes: a guide for children, adolescents, young adults and their caregivers. New York: Marlowe & Company; 2005.